Note to reader

This draft version of Chapter 1 in the Technical Background Report to the Global Mercury Assessment 2018 is made available for review by national representatives and experts. The draft version contains material that will be further refined and elaborated after the review process. Specific items where the content of this draft chapter will be further improved and modified are:

1. All graphics will be redrawn to a common appearance from the originals presented here, with their sources cited in the captions.
2. References will be completed and presented in a uniform style.
3. Conclusions and main messages will be formulated

GMA 2018 Draft Chapter 1 Introduction. Peter Outridge, Robert Mason, Feiyue Wang, Lars-Eric Heimburger, Milena Horvat, Xinbin Feng, Simon Wilson

18

19 # Contents

29

30

31

32

33

Chapter 1 Introduction

1.1 Background and Mandate

This report constitutes the Technical Background Material to the Global Mercury Assessment 2018 (GMA 2018). The GMA 2018 has been prepared in response to a request issued by UNEP's Governing Council (now UN Environment Assembly) that UN Environment should update its 2013 Global Mercury Assessment (GMA 2013) within a period of 6 years, i.e. for delivery no later than 2019. This Technical Background report is developed as a joint project by UN Environment and the Arctic Monitoring and Assessment Programme (AMAP).

The GMA 2018 provides a scientific assessment of Hg emissions and releases, and its transport of fate in the global environment. The report reflects progress made by the scientific community, national authorities and organisations in better understanding atmospheric Hg emissions (Chapter 2), Hg levels in air (Chapter 3), atmospheric transport and fate (Chapter 4), releases to water (chapter 5), and the cycling and methylation of Hg in the aquatic environment (Chapter 6). In addition to updating the GMA 2013, this report includes additional, new sections on observed levels of Hg in biota (Chapter 7), and observed levels and effects of Hg in humans (Chapter 8).

1.2 Recent advances in understanding of global mercury cycling

1.2.1 A General Overview

Owing to the scale and chemical complexity of Hg in the global environment, and the lack of detailed information for many parts of the Hg cycle, the planetary Hg cycle is best described and communicated in a quantitative manner by using the outputs from global-scale models, the subject of this section. In general, Hg is released into the global environment from natural sources and processes such as volcanoes and rock weathering, and as a result of human activities. Once it has entered the environment, Hg cycles between the major environmental compartments – air, soils and waters – until it is eventually removed from the system through burial in deep ocean sediments and mineral soils (Fig. 1.2.1). Only a minute fraction of the Hg present in the environment is in the most toxic and bioavailable form - monomethylmercury (MeHg). Monomethylmercury is produced from inorganic Hg mainly in aquatic ecosystems through natural microbiological processes. The natural processes responsible for the formation and destruction of MeHg are only partly understood, which contributes to the difficulties in predicting the direct positive effects of regulatory action on biological Hg concentrations and human

exposure. However, regulatory action can only work to reduce anthropogenic Hg inputs into the environment. Recent findings on the methylation/ demethylation part of the Hg cycle are presented in Chapter 6.2.

In the 2013 Global Mercury Technical Assessment (AMAP/UNEP, 2013), based on a global model and budget developed by Mason et al. (2012), it was estimated that over the past century anthropogenic activities cumulatively have increased atmospheric Hg concentrations by 300-500%, whereas Hg in surface ocean waters less than 200 metres deep has increased on average by ~200%. Deeper waters exhibit smaller increases (11-25%) because of limited exposure to atmospheric and riverine anthropogenic Hg inputs, and the century- to millennium-scale residence times of these slowly over-turning, isolated water masses. Because of the naturally large Hg mass present in soils, the average Hg increase is only ~20% in surface organic soils and is negligible in mineral soils.

As with almost all modelled global budgets of trace elements and chemical substances, large uncertainties exist regarding the amounts of Hg 'stored' in different environmental compartments, the fluxes of Hg between them, and the rates of removal of Hg from the biologically active parts of the global environment (AMAP/UNEP, 2013). These uncertainties limit confidence in our understanding of the Hg cycle and in our ability to predict the responses of ecosystem Hg concentrations to changes in emissions due to international regulatory actions. Therefore, major on-going efforts have been mounted to reduce these uncertainties and derive a more robust, accurate global model.

Since 2012, additional measurements of Hg concentrations and fluxes in oceans, atmosphere and soils have led to suggested refinements of global budgets and models by several research groups (Table 1.2.1), but major uncertainties persist. In general, the new estimates of Hg in the atmosphere mostly agree within the limits of uncertainty with the AMAP/UNEP (2013) budget. However, two of the recent studies (Amos et al., 2013; Zhang et al., 2014) suggest that the terrestrial system contains a larger fraction of anthropogenic Hg compared to the oceans than was previously believed. This revision is supported by new modelling of the global transport and fate of atmospheric gaseous elemental mercury (GEM) (Song et al., 2015). Also, recent work on atmospheric Hg dynamics under forest canopies suggests that the uptake of GEM through leaf stomata at night-time has previously been significantly underestimated, and that GEM-containing litterfall and throughfall in global vegetation, and not wet and dry deposition of Hg^{II} species, may represent the largest net flux of atmospheric Hg to terrestrial ecosystems (Fu et al., 2016; Wang et al., 2016; Obrist et al., 2017).

With respect to the world's oceans, there are significant differences between the new models concerning the quantity of anthropogenic Hg presently circulating in seawater (c.f. Amos et al., 2013, 2015; Zhang et al., 2014; Lamborg et al., 2014). Because much of the current risk from Hg to human and wildlife is derived from marine food-webs, the questions of how much anthropogenic Hg is present in the oceans, its distribution, and its rate of clearance from seawater, are of fundamental importance and so are the main focus of section 1.2.

The observed differences between models concerning these questions are primarily due to varying estimates of the amount and environmental fate of atmospheric emissions from historical mining in the Americas between the 15thand late 19thcenturies, and to differences in the estimated amount of natural Hg originally present in the oceans (see Table 1.2.1). Overall, the different chemical rate constants used for modelling circulation processes within and between oceanic, atmospheric and terrestrial compartments are a secondary factor in uncertainty. Substantial Hg releases to land, freshwaters and air occurred from primary Hg mineral mining, and gold (Au) and silver (Ag) mining and amalgamation, in South/Central America during the Spanish colonial period (ca. 1450-1850 AD), and later from North American artisanal and small-scale Au and Ag mining during the "Gold Rush" era (ca. 1850-1920) (Nriagu, 1993; Strode et al., 2009). It is generally agreed that some fraction of the Hg from these historical emissions is still circulating within the global environment, and that this has had an effect on present-day environmental Hg levels, especially in the oceans. But quantification of that effect is currently uncertain.

Table 1.2.1. Recent estimates of total, anthropogenic and "natural"[a] Hg in global air, soils and oceans (units in kilotonnes (1 kt = 1,000 t)).

	Amos et al. (2013)	Zhang et al. (2014)	Lamborg et al. (2014)	Mason et al. (2012); AMAP/UNEP (2013)
Atmospheric Hg				
Total	5.3	4.4	n/a	5.1
Anthropogenic	4.6	3.6		3.4-4.1[b]
Natural	0.7	0.8		1.0-1.7
Soil Hg				
Total	271	--	n/a	201
Anthropogenic	89	92		40
Natural	182	--		161
Oceanic Hg				
Total	343	257	316	358
Anthropogenic	222	66 (38-106)[c]	58±16[d]	53
Natural	122	191	258[e]	305

[a] – The time point for designation of the "natural" Hg states, and therefore the quantification of "natural" and "anthropogenic" Hg masses, differed between studies: specified at 2000 BC in the "pre-anthropogenic period" by Amos et al. (2013), at 1450 AD by Zhang et al. (2014) which was prior to major historical mining, and *ca.* 1840 AD by Lamborg et al. (2014) which was prior to the North American "Gold Rush" and the expansion of coal-fired combustion sources. The anthropogenic Hg values from Mason et al. (2012) are based on increases over the last century, and thus their "natural" Hg mass may be over-estimated and the anthropogenic mass under-estimated compared with the other studies.

[b] – Ranges for anthropogenic and "natural" Hg calculated assuming an estimated 300-500% increase in total Hg due to anthropogenic activities over past century (Mason et al. 2012).

[c] - the Zhang et al. (2014) best estimate for oceanic anthropogenic Hg is followed by its uncertainty range in brackets.

[d] - based on an oceanic anthropogenic Hg:anthropogenic CO_2 ratio for 1994; a more recent (higher) oceanic CO_2 estimate gave an Hg_{anthr} estimate of 76 kt Hg (Lamborg et al., 2014).

[e] – calculated by subtraction.

1.2.2 How much anthropogenic Hg is in the world's oceans, and what was its source?

The total amount of Hg currently in oceans reflects a mixture of sources: historical anthropogenic inputs to air, land and oceans; historical natural emissions; and current year anthropogenic and natural releases. Consequently, global models need to estimate these quantities and how they have been cycled, transported and transformed over long (decadal to century) time-scales.

Up until 2012, the published estimates of oceanic anthropogenic Hg exhibited more than an order of magnitude range, from 7.2 to 263 kt (Mason et al., 1994; Lamborg et al., 2002; Sunderland and Mason, 2007; Selin et al., 2008; Strode et al., 2010; Soerensen et al., 2010; Streets et al., 2011; Mason et al. 2012). Since then, another estimate (222 kt) near the upper end of this range was derived by Amos et al. (2013) based on Streets et al. (2011) putative history of major emissions from historical Ag and Au mining activities. Subsequently, however, Zhang, Streets and colleagues (Zhang et al., 2014) revised the historical mining emissions downwards by three-fold to make the trends in global Hg emissions more compatible with the Hg deposition histories recorded in 120 lake sediments world-wide (Figure 1.2.2).

The revision was stimulated in part by a historical analysis of documented liquid elemental Hg importation and consumption during Ag mining operations in the 15-17th centuries in what is today Mexico, Peru and Bolivia (Guerrero, 2012). In the AMAP/UNEP 2013 report, it was estimated that 45% of the Hg used in artisanal gold mining and amalgamation in the present-day was volatilized into the atmosphere. By comparison, Guerrero (2012) suggested that only 7-34% was volatilized during historical Ag production, with 66-93% of the consumed Hg forming solid calomel (Hg_2Cl_2) that was trapped in mining waste and deposited locally into streams or landfills. This new study of historical Ag production is a potentially important advance in understanding of the global Hg cycle, because another recent estimate of cumulative global atmospheric Hg emissions from all man-made sources up to 2010 suggested that Ag production was the largest single source of Hg, contributing several-times more Hg to air throughout history (146 kt, 31% of total) than large-scale and artisanal gold production combined (55.4 kt; Streets et al. 2017). Emissions from Ag production are thought to have peaked during the late 19th century, coincident with North American mining, however, there are relatively large uncertainties of up to 100% (represented in terms of 80% confidence intervals) around the total emissions for the period 1870-1910 (Streets et al. 2017).

After assuming that historical Ag and Au mining and amalgamation had the same loss rate to the atmosphere (17%), Zhang et al.'s (2014) revised anthropogenic emission inventory (see Fig. 1.2.2) was

markedly smaller than that of Streets et al. (2011) (cumulative totals of 190 kt versus 351 kt, respectively). Using this revised inventory with the GEOS-Chem model, Zhang et al. (2014) found a 3-fold lower current oceanic anthropogenic Hg mass than that derived by Amos et al. (2013) using the same model but a larger emission from historical mining (see Table 1.2.1).

Corroborative data supporting the lower historical mining emissions proposed by Zhang et al. (2014) came from an independent analysis of another large global set of lake sediment Hg profiles (Engstrom et al. 2014). Atmospheric Hg deposition was substantially increased during the Spanish colonial period in one South American lake (Negrita) close to the sites of historical mining and amalgamation activities, with less impact in another regional lake (El Junco) further away (Fig. 1.2.3). But no evidence of increased deposition at this time was found in sediment cores from remote North American or African lakes (see Fig. 1.2.3), suggesting that the historical contamination from Spanish colonial mining was geographically limited to surrounding terrestrial and freshwater ecosystems. Thus, the world-wide lake sediment record indicates a large local, but negligible global, impact from Spanish era Au and Ag mining and production during the 15th to 17th centuries.

Amos et al. (2015) discounted this evidence by arguing that lake sediments in general respond relatively slowly and insensitively to changes in atmospheric Hg deposition. Recent evidence of significant GEM uptake by plant leaves, and of high Hg fluxes to soils in leaf litterfall and throughfall (Fu et al., 2016; Obrist et al., 2017), raises another complicating possibility - that sediment archives ultimately may be more reflective of trends in GEM concentrations, through transfer from watersheds via litterfall and throughfall, rather than of wet and dry deposition. Amos et al. (2015) also proposed that the Guerrero (2012) volatilization estimate was unrealistically low because it omitted Hg losses during amalgamation, reprocessing of Hg-containing Ag and Au products, and revolatilization from historic solid mining wastes. Evaluation of alternative GEOS-Chem model scenarios by Amos et al. (2015) suggested that the "mining reduced 3x" history of Zhang et al. (2014) was inconsistent with Hg measurements in present-day environmental reservoirs, as well as with the magnitude of Hg enrichment in peat and some lake sediment archives. However, examination of the published model outputs shows that the reduced mining scenario gave markedly closer agreement with observed upper ocean total Hg concentrations and net oceanic evasion rates than the original mining emission history of Streets et al. (2011), with almost identical present-day soil Hg concentrations and net terrestrial flux (see Amos et al. (2015), c.f. Figs. 3d, 3g, 3f, 3h, respectively).

Independent evidence supporting the revised (lower) Zhang et al. (2014) emission history, and the lake sediment records of Engstrom et al. (2014), was recently provided by three remote glacier ice core records from the Yukon, Greenland, and Tibetan Plateau (Fig. 1.2.4). Streets et al. (2011) estimated there to have been an average ~500% increase in primary anthropogenic emissions globally between 1850 and the late 1800s that was attributable to the North American Gold Rush. However, the two Arctic or sub-Arctic glacier records (Mount Logan, Yukon (Beal et al., 2015), and the NEEM site, Greenland (Zheng, 2015)) reported increases in mean Hg accumulation rate of only 120% and 30%, respectively, between 1748-1850 and 1851-1900. The ice core from Tibetan Plateau (Mount Gelaidandong, ~6620 m.a.s.l.; Kang et al., 2016) did not display any marked increase in Hg accumulation in the late 1800s that could be due to large, globally-distributed emissions from the North American Gold Rush (see Fig. 1.2.4). Furthermore, neither the Mt. Logan core, which extended back to ~1400 AD, nor the Mt. Gelaidandong core, which extended back to 1477 AD, revealed elevated Hg accumulation during the 15th to 17th centuries that could be attributed to the Spanish Colonial Ag and Au mining operations in Central America and Mexico. In both glacier cores, by far the highest Hg accumulation rates over the last ~600 years occurred after the 1920s (Beal et al., 2015; Kang et al., 2016). In summary, all three ice core records are in closer agreement with the downwards-revised historical emissions budget of Zhang et al. (2014) than with the earlier estimate by Streets et al. (2011) which underpinned Amos et al.'s (2013) global model.

Thus, the weight of evidence at present supports the Zhang et al. (2014) emission history, and suggests that the atmospheric Hg emissions produced by historical mining and amalgamation techniques were geographically restricted, with dispersion confined mostly to local and regional terrestrial and freshwater environments. That these historical emissions had significant effects on Hg levels in areas around the mining operations is not in dispute. Other studies have shown marked local or regional contamination of lake sediment and glacial ice archives by historical Ag/Au mining (e.g., Schuster et al., 2002; Cooke et al., 2009; Correla et al., 2017). However, current evidence supports the interpretation that historical mining had less impact on globally-distributed atmospheric emissions and deposition than coal combustion and other high temperature industrial emissions had in the 20th century. Commercial Hg-containing products have also been suggested to be significant contributors to global Hg releases to air, soil and water from the late 1800s onwards (Horowitz et al., 2014). Overall, the recent revised emissions estimates, and archival records of deposition, support the prevailing paradigm that present-

day atmospheric deposition rates are 3- to 5-fold higher than during the pre-industrial period (i.e. from 1450 to 1850) (Engstrom et al., 2014; Lamborg et al., 2014; Zhang et al., 2014).

Nonetheless, the cumulative impacts of historical mining over four centuries on the current oceanic (and terrestrial) anthropogenic Hg inventory have been substantial. Zhang et al. (2014) calculated that about 67% of the cumulative anthropogenic Hg emissions to air throughout history (130 out of 190 kt) was due to precious metal mining, with 21% (40 kt) due to coal combustion and 11% (20 kt) from other industrial activities. Zhang et al. (2014) also calculated that most of the anthropogenic Hg mass in today's oceans (44 kt out of 66 kt) was deposited between 1450 and 1920 due to the emissions from historical Ag/Au mining, with the remaining one-third coming from predominantly coal-based emissions since 1920. The total anthropogenic mass in today's oceans (66 kt) estimated by Zhang et al. (2014) is in good agreement with another recent estimate of oceanic anthropogenic Hg (58±16 kt; Lamborg et al., 2014) derived using a completely different methodology based on seawater Hg concentration profiles combined with anthropogenic CO_2 and remineralized phosphate as proxies for oceanic Hg distribution. That two studies, using different approaches, arrived at similar estimates increases confidence in the robustness of their conclusions. Both of these recent estimates fall within the lower half of the previous range of values and are close to the Mason et al. (2012) estimate of 53 kt used in AMAP/UNEP (2013) (see Table 1.2.1).

Inconsistencies remain in the evidence pertaining to the actual rates of atmospheric historical mining emissions that impacted the global atmosphere and oceans. Although the 3-fold reduction in mining emissions by Zhang et al. (2014) brought their modelled emission history during the late 19th and early 20th centuries closer to global lake sediment flux patterns, compared with the Streets et al. (2011) inventory, the emissions pattern remained elevated compared to lake sediment trends during the same period (see Fig. 1.2.2). Also, the estimate for cumulative pre-1920 anthropogenic emissions by Zhang et al. (2014; i.e., 67% of the total) is several times larger than the Mt. Logan ice core results reported by Beal et al. (2015; in which only 22% of total accumulated Hg was deposited prior to 1900), and the Mt. Gelaidandong study by Kang et al. (2016; see above). It may be that a further reduction in the assumed proportion of volatilized Hg from historical mining/amalgamation would bring the emission history and the remote lake sediment and ice core records into even closer agreement.

1.2.3 Where is anthropogenic Hg distributed in the environment, especially the oceans?

The Zhang et al. (2014) global model projected that in the current global environment, 2% (3.6 kt) of the all-time cumulative anthropogenic emissions remains in the atmosphere, 48% (92 kt) is held in soils, and 50% (94 kt) in the oceans - 35% (66 kt) in seawater, and 15% (28 kt) buried in ocean sediments. For the oceans, atmospheric deposition from current primary emissions as well as revolatilization of legacy emissions contributes over 90% of the total (atmosphere + rivers) Hg inputs (4.0 out of 4.3 kt/yr; Fig. 1.2.5), with riverine inputs that reach the open ocean comprising a minor fraction (6%, 0.3 kt/yr.). Amos et al. (2014) estimated a substantially higher riverine contribution (1.5±0.8 kt/yr.; 30% of total 5.2 kt/yr. inputs) to the open ocean based on an observational database of riverwater Hg concentrations and consideration of river-offshore transport efficiencies for different estuary types. Most (72%) of the riverine Hg entering into estuaries was scavenged and deposited into coastal marine sediments (Amos et al., 2014). By comparison, Mason et al. (2012) arrived at an estimate of 0.38 kt/yr. from rivers, which comprised ~10% of total ocean inputs. Recent data from Chinese rivers (Liu et al., 2016) support the lower estimates of Mason et al. (2012) and Zhang et al. (2014).

Significant differences exist between recent models in their portrayal of the vertical distribution of oceanic anthropogenic Hg because of the above-mentioned variance in historical emission estimates and different assumptions about the penetration rate of anthropogenic Hg into deep ocean waters. Zhang et al. (2014) and Lamborg et al. (2014) largely agreed in their relative distribution, except that the deep ocean (below 1000 m depth) contained proportionally more anthropogenic Hg in Zhang et al.'s (2014) simulation (45% of total oceanic anthropogenic Hg, vs 35% in Lamborg et al. (2014)). Compared to Zhang et al. (2014), Streets et al. (2011) and Amos et al. (2013) calculated similar increases in the anthropogenic Hg content of the surface ocean (4.4 times natural concentrations, vs. 3.6-5.9 times, respectively), but larger increases in the thermocline/intermediate depths (1.2 times, vs 2.7-5.3 times) and deep ocean (1.2 times, vs. 1.5-2.1 times). In addition to their adoption of larger historical mining emission estimates, Streets et al. (2011) and Amos et al. (2013) assumed faster vertical mixing rates compared with the other two studies.

Large inter-basin differences in the distribution of anthropogenic Hg were also apparent in intermediate and deep ocean waters, but were relatively uniform in surface waters, in the modelling of Zhang et al. (2014) (Fig. 1.2.6). Vertical and horizontal advection of Hg inputs to the ocean which reflect ocean currents and areas of deep water formation, and high biological productivity and rapid particle scavenging of dissolved Hg in some tropical seas, account for the inter-basin patterns.

1.2.4 What are the implications of different models for the rate of clearance of anthropogenic Hg from the world's oceans?

The differences between models and their underpinning historical mining emission estimates are associated with significant differences in implied response times of the oceans to emission reduction scenarios. All global ocean-atmosphere models predict that Hg clearance rates from most ocean basins will be slow relative to the rate of anthropogenic emission reductions in future, such that removal of anthropogenic Hg from the world's oceans will take many decades to centuries depending on the ocean basin and depth interval of the water mass in question, as well as the trajectory of emission controls (Mason et al., 2012; Lamborg et al., 2014; Zhang et al., 2014; Amos et al., 2015). But according to Selin (2013) and Engstrom et al. (2014), the "high emission" scenario of Streets et al. (2011) and Amos et al. (2013, 2015) suggests much slower and delayed reductions in environmental Hg levels than other models, especially in the oceans, following emission curbs. Even at current global emission levels, there exists a general scientific consensus that seawater and marine food chain Hg levels are likely to substantially increase, because of the slow clearance rate of legacy Hg from the world's oceans coupled with additional legacy anthropogenic Hg released from soil profiles into rivers and revolatilized into the air (Sunderland and Selin, 2013).

Until current significant deficiencies in our understanding of marine Hg cycling, and the rates of transformation between species that influence the major sinks for ocean Hg (evasion to the atmosphere and burial in sediments) are resolved, and greater consistency is achieved in the interpretation of various natural archive recorders of Hg deposition from the atmosphere, the prediction of the timeline and effects of global emission reductions will remain uncertain. It is clear, however, that irrespective of these scientific uncertainties, emissions reductions are required as soon as possible to reverse the trend in oceanic anthropogenic Hg back towards natural levels because of the long response time of the ocean to changes in inputs (Selin 2013; Sunderland and Selin, 2013; Engstrom et al., 2014).

1.2.5 What are the main uncertainties in global Hg models and budgets?

Here we summarize the knowledge gaps and recommendations for further research from a number of recent papers (Amos et al., 2013; Engstrom et al., 2014; Zhang et al., 2014, 2016; Lamborg et al., 2014, 2016; Song et al., 2015). Scientific uncertainties can be grouped under two headings: natural inputs and processes, and anthropogenic emissions. Under the former category can be listed:

- Removal rates of anthropogenic Hg from the surface ocean are the net result of competition between three simultaneously occurring natural processes: particulate flux from the surface to the deep ocean (the "biological pump", involving particle scavenging and settling); the mixing of surface and deep-ocean waters; and the reduction of inorganic Hg^{II} and subsequent evasion of Hg^0 back into the atmosphere. Further coupled ocean-atmosphere measurement studies are needed to comprehensively measure the concentrations of various Hg species spatially and temporally, and to better understand the transport and transformation rates of these processes. The need is particularly acute in the Southern Hemisphere open oceans, as well as in regions where elevated anthropogenic Hg concentrations can be expected, such as the eastern equatorial Atlantic, eastern equatorial and high latitude Pacific, and northern Indian Oceans.
- Related to the latter effort, uncertainties in the robustness of measurements of atmospheric and seawater Hg concentrations are exacerbated by relatively large inter-laboratory comparison errors. Few inter-comparison efforts have been mounted (e.g. Gustin et al., 2013 for atmospheric Hg^0 determinations); there is a particular need improve the overall reliability of seawater Hg measurements. Past intercalibration exercises have only addressed total Hg and total methylated Hg in seawater, and the results indicated significant discrepancies amongst the participating laboratories. Future intercalibration exercises should continue the effort of attaining reliable total Hg and MeHg measurements, and be extended to all Hg species including unstable species such as dimethyl Hg and dissolved Hg^0. The development of suitable seawater reference materials is encouraged.
- The role of natural inputs in the global Hg budget is poorly constrained but potentially is of primary importance. If the actual rate of emissions from natural sources is markedly higher than currently believed, it would undermine current assumptions about the absolute amounts of, relative balance between, natural and anthropogenic sources which are fundamental to modelling efforts and to our understanding of the global Hg cycle.

Present estimates of global volcanic Hg emissions to air range over three orders of magnitude (0.1 – 1000 t/yr.) (Nriagu, 1989; Ferrara et al., 2000; Pyle and Mather, 2003; Nriagu and Becker, 2003; Bagnato et al., 2014). For oceans, the AMAP/UNEP (2013) report assigned a value of <600 t/yr. total Hg input from hydrothermal vents, which was based on few data and no systematic studies. Two recent Geotraces cruises sampled waters around hydrothermal vents in the North Atlantic and

equatorial Pacific Oceans (Bowman et al., 2015; 2016). In the North Atlantic, the plume of elevated Hg concentration around the vent was highly developed and extended vertically over a depth of around 1000 m and for 1000 km away from the ridge crest (Bowman et al. 2015). In contrast, there was no strong evidence for a plume over the East Pacific Rise in the equatorial Pacific (Bowman et al., 2016). These results further indicate that there is a substantial difference in the extent of Hg inputs from different hydrothermal sources. Overall, there is not sufficient new information to update the estimate of hydrothermal inputs made in 2013, although this may be the single most important primary natural Hg source to the global Hg cycle (Sonke et al. 2013). In order to make direct estimations for global hydrothermal Hg fluxes, more observations of (focused and diffuse-flow) vent fluids and hydrothermal plumes are needed to better constrain the Hg flux, and its contribution to the global Hg cycle (German et al. 2016). In addition, submarine groundwater discharges are likely to bring important amounts of Hg into the ocean, which global models do not account for. Several recent papers indicate that Hg inputs *via* submarine groundwater are as large as atmospheric inputs, at least in coastal environments (Bone et al. 2007, Laurier et al. 2007, Black et al. 2009, Lee et al. 2011, Ganguli et al. 2012).

- Given the importance of terrestrial soils as possibly the largest repository of legacy anthropogenic Hg, global budget calculations will benefit from better understanding of terrestrial Hg cycling including measurements of the evasion rates of deposited Hg from soils, and release rates of Hg to water following degradation of soil organic matter.

In terms of anthropogenic emissions, the absolute amounts of historical emission inventories, especially the role of precious metal mining, has been called into question by recent work comparing model outputs with past Hg deposition rates reconstructed from natural archives of atmospheric deposition (see Zhang et al. 2014, c.f. Amos et al., 2015). Some of the uncertainty lies with the natural archives. For example, a recent paper has shown that the Hg accumulation rates in a Tibetan Plateau glacier ice core were 1 to 2 orders of magnitude lower than in a nearby lake sediment, yet the two archives yielded remarkably similar trends (Kang et al., 2016). While the agreement in trends is encouraging, the difference in absolute values begs the question of what is the most reliable quantitative estimate of past atmospheric deposition. Amos et al. (2015) concluded that peat bog cores gave more accurate reconstructions than most lake sediment cores. Given the now-apparent importance of historical emissions to current world Hg budgets and to future emission reduction scenarios, and the significant

differences in the natural archive records of those emissions, a concerted effort to understand the reasons for the different conclusions from peat, lake sediment and glacial ice archives is called for. Arriving at an agreed historical emission figure from precious metal mining would eliminate a large degree of the uncertainty surrounding current anthropogenic Hg inventories in soils and the oceans.

The accuracy of the recent global emission inventories, including that in AMAP/UNEP (2013), has been questioned in part because of the inconsistency between the recent trends in emission inventories, which are flat or increasing, and the large (~30-40%) decreases in atmospheric GEM and wet deposition since 1990 at background Northern Hemisphere monitoring stations (Zhang et al., 2016). The latter authors found that the emissions and GEM trends could be brought into closer agreement by accounting for the decline in Hg release from commercial products over this period, by reducing the atmospheric revolatilization rate of Hg from present-day artisanal and small-scale gold mining, and by accounting for the shift in Hg^0/Hg^{II} speciation of emissions from coal-fired utilities after implementation of gaseous pollutant control measures. Because the emission inventories are the basis of global modelling efforts, resolving this discrepancy will improve the accuracy of global budgets and future trend scenarios. ASGM emissions were the largest single anthropogenic source of atmospheric Hg in AMAP/UNEP (2013), but this finding has been disputed (Engstrom et al., 2014; Zhang et al., 2016). Verifiable and higher quality emission data from ASGM operations are therefore a priority need.

The global models and an improved understanding of the global Hg cycle are important for our capacity to predict how regulatory efforts to reduce current emissions to air, water and land will affect concentrations in environmental compartments, biota and human exposure. The large uncertainties and identified knowledge gaps described above should not be taken as a sign that regulatory action is not needed or can be delayed until the large research efforts have led to a reduction of these uncertainties. All models and evaluations based on field measurements are in agreement that current anthropogenic emissions of Hg lead to increased environmental exposure of wildlife and humans (albeit of varying magnitude) and that reducing these emissions is a necessity for reducing the negative environmental impacts of Hg. The uncertainties and knowledge gaps are mainly affecting our capability to predict where and when the environment will respond to reduced emissions, not if it will.

392

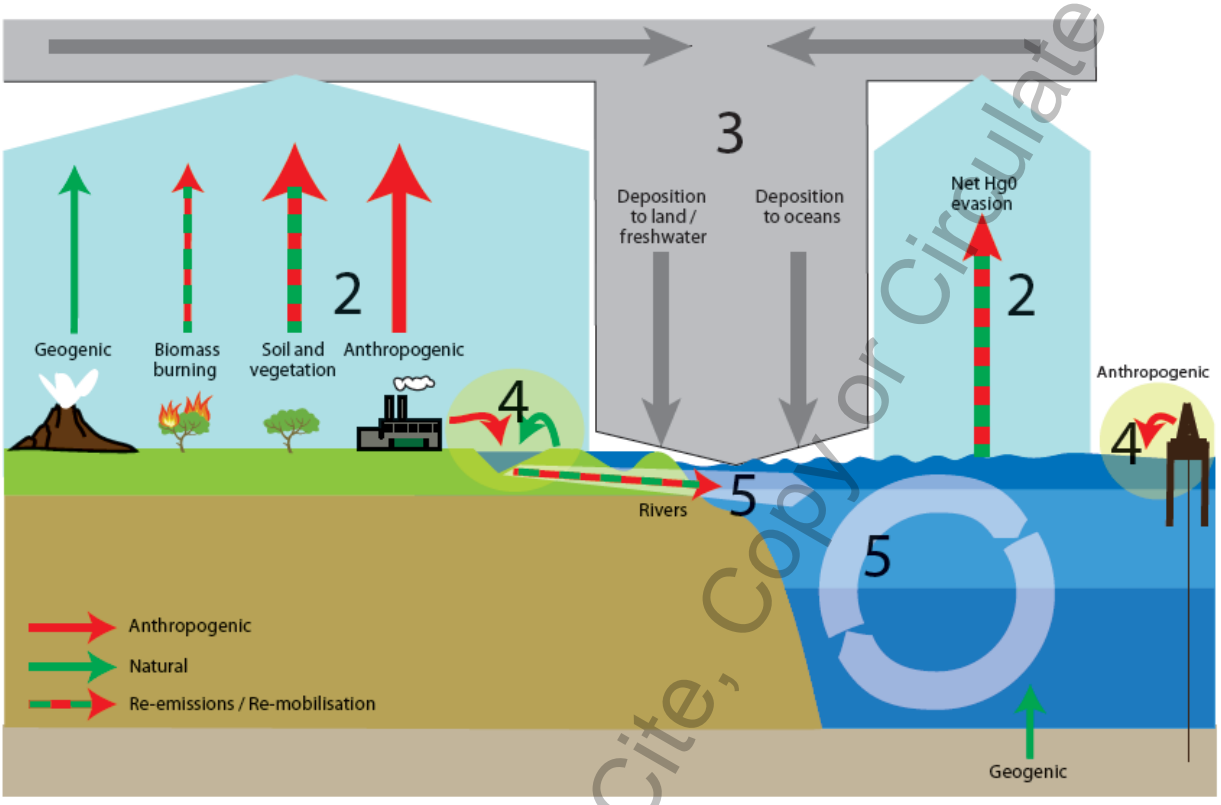

393

394 Figure 1.2.1 Summary diagram of global movements of total mercury between air, soils and oceans
395 (source: AMP/UNEP 2013). Figure to be redrafted (remove chapter numbers, add deposition into
396 mineral soils and deep ocean sediments, deposition arrows to land and oceans need to be mixed
397 red/green colour, remove marine oil well symbol).

398

399

400

401

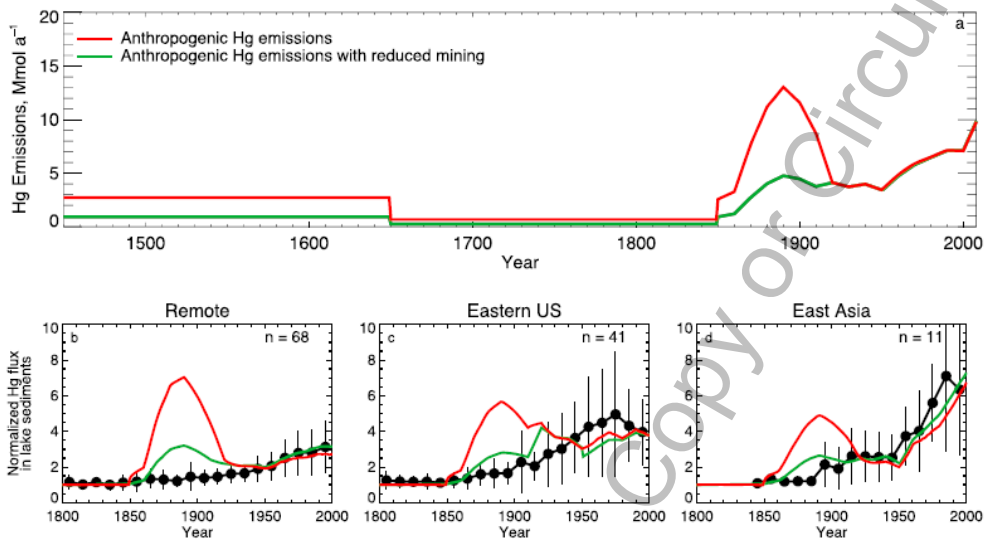

Figure 1. Historical trends in anthropogenic Hg emissions and Hg accumulation flux to lake sediments. (a) Global anthropogenic Hg emissions between 1450 and 2008. The emission inventory from Streets et al. (3) is shown in red, while the emission inventory with mining emissions reduced by a factor of 3 is shown in green. Mean historical Hg flux inferred from sediment cores in (b) 68 remote lakes, (c) 41 lakes in the eastern U.S., and (d) 11 lakes in East Asia. All the fluxes are normalized to 1800–1850 levels. Observations (black filled circles with vertical line showing 1σ) are compared against model results (red and green lines correspond to the original and reduced mining inventories, respectively).

402

403 Figure 1.2.2. Revision of global anthropogenic Hg emission history based on a three-fold reduction in

404 mining emissions from 1450 to ~1920 AD. (Source: Zhang et al. 2014).

405 [figure to be redrawn, and caption revised using Zhang's caption, if this fig is used)

406

407

408

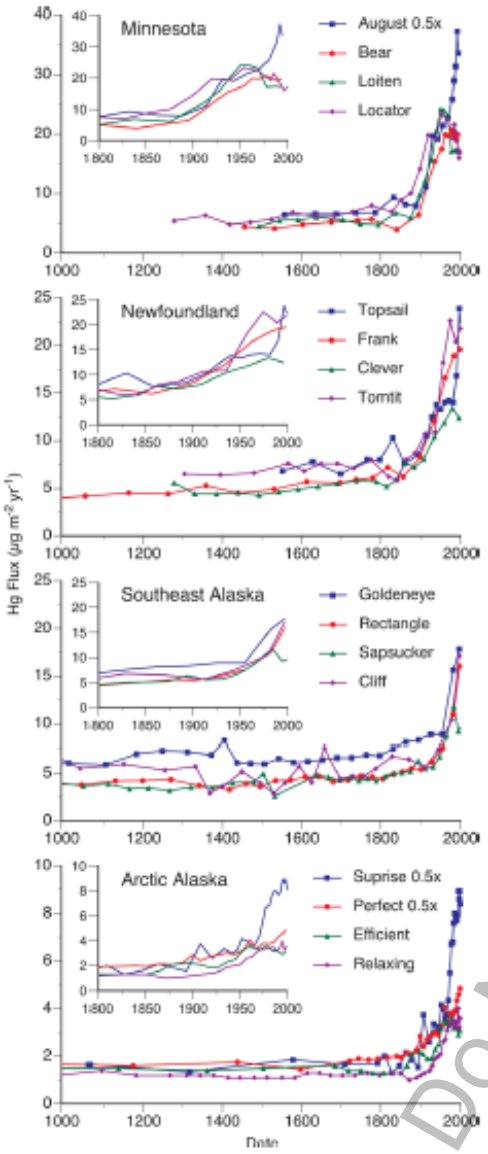

Figure 1. Hg accumulation trends in sediment cores from remote North American lakes. Fluxes scaled by 0.5× for August, Surprise, and Relaxing lakes. Insets show detail for most recent 200 years.

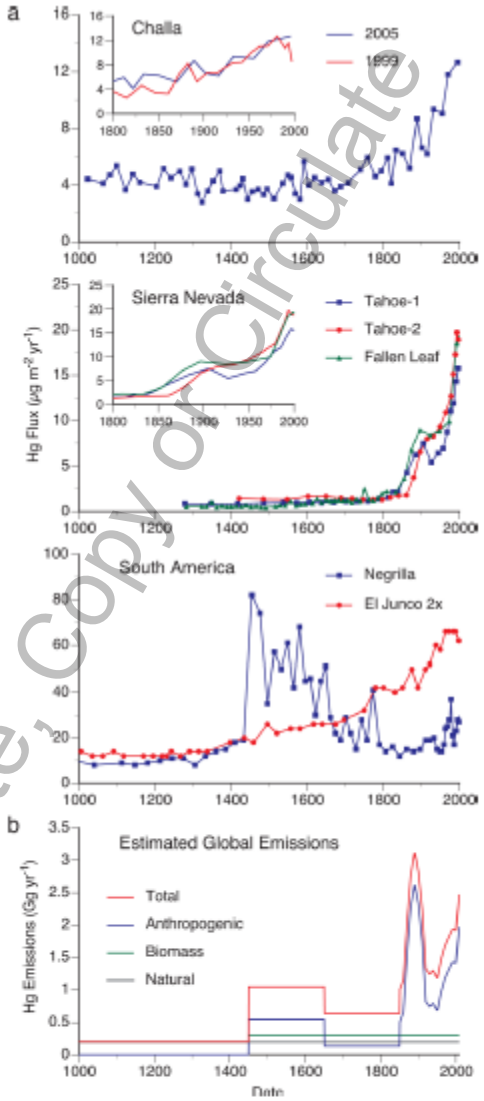

Figure 2. (a) Hg accumulation trends in sediment cores from Lake Challa (Kenya/Tanzania), El Junco and Negrilla (S. America), and Tahoe and Fallen Leaf (Sierra Nevada). Insets show detail for most recent 200 years. The two cores shown for Lake Challa were collected in 1999 and 2005 from nearby locations,[36] while the two cores from Lake Tahoe were collected from different parts of the basin.[33] (b) Primary Hg emissions as estimated by Streets et al.[15]

Figure 1.2.3 Historical Hg fluxes in global lake sediments. From Engstrom et al. 2014 ES&T. [figure to be redrawn, and caption revised using Engstrom's caption, if this fig is used)

418

419

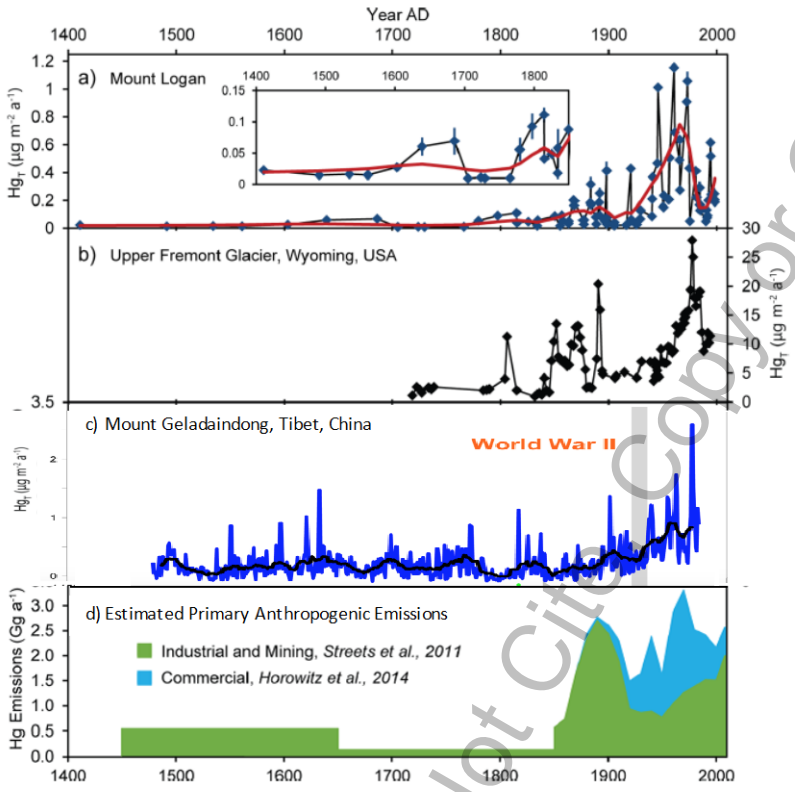

Figure 3. Multicentury Hg_T records from ice cores compared with estimates of primary anthropogenic emissions used in recent global Hg models. (a) Mount Logan Hg_T fluxes (blue points) with 1σ error bars, LOESS smoother (red line), and inset with adjusted *y*-axis for the Preindustrial Period. (b) Hg_T fluxes in the Upper Fremont Glacier ice core calculated using an assumed constant accumulation rate of 800 kg m^{-2} a^{-1} modified from Schuster et al.[1] (c) Geladaindong Glacier HgT fluxes (bars) with the 15-year running average (blue line) (Kang et al., 2016). (d) Estimated primary anthropogenic Hg emissions from industrial and mining sources modified from Streets et al.,[7] and additional

420

421 Figure 1.2.4. Glacial ice core records of atmospheric Hg deposition from Mount Logan, Yukon (source:
422 Beal et al., 2016), the Upper Fremont Glacier, Wyoming, USA (source : Beal et al. 2015) and Mount
423 Geladaindong, Tibetan Plateau, China (source: Kang et al., 2016), compared with the suggested global
424 atmospheric emission since 1450 AD by Streets et al. (2011).

425 [figure source from Beal et al 2016, to be redrawn, and caption revised using Beal's caption, if this fig is
426 used]

427

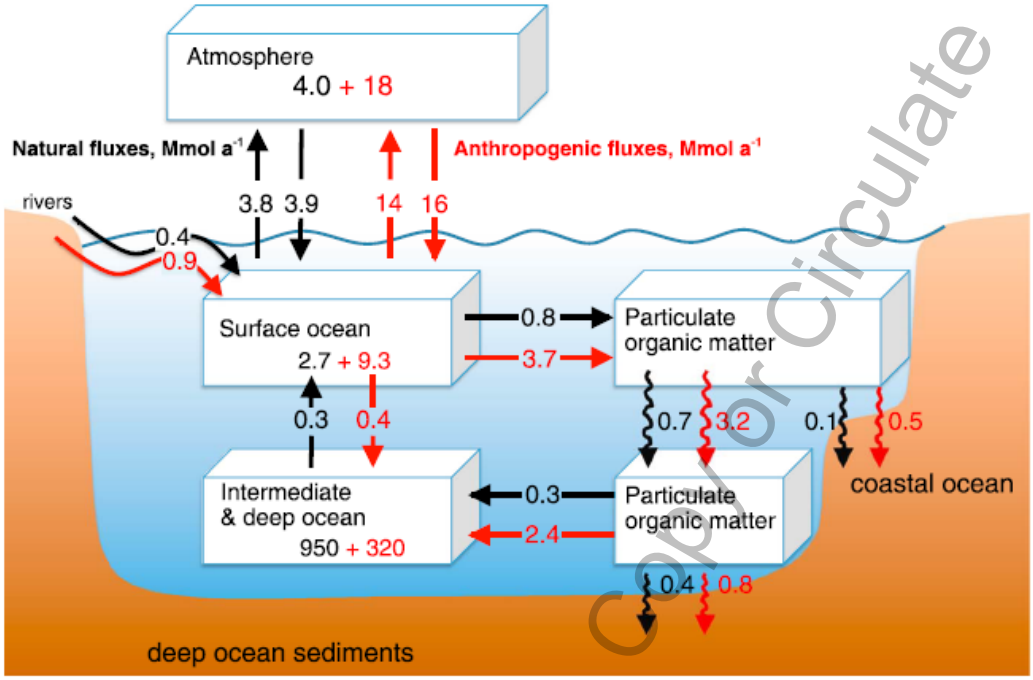

Figure 5. Human influence on the marine Hg cycle. The numbers in the boxes correspond to the mass of Hg in each reservoir (in units of Mmol), while the arrows indicate fluxes in Mmol a^{-1}. The preanthropogenic conditions are in black arrows and numbers, while the human perturbation is shown in red.

428

429 Figure 1.2.5. Natural and anthropogenic Hg inputs and masses in the world's oceans. from Zhang et al.

430 2014 GBC (to be redrawn, and Mmol units converted into kilotonnes).

431

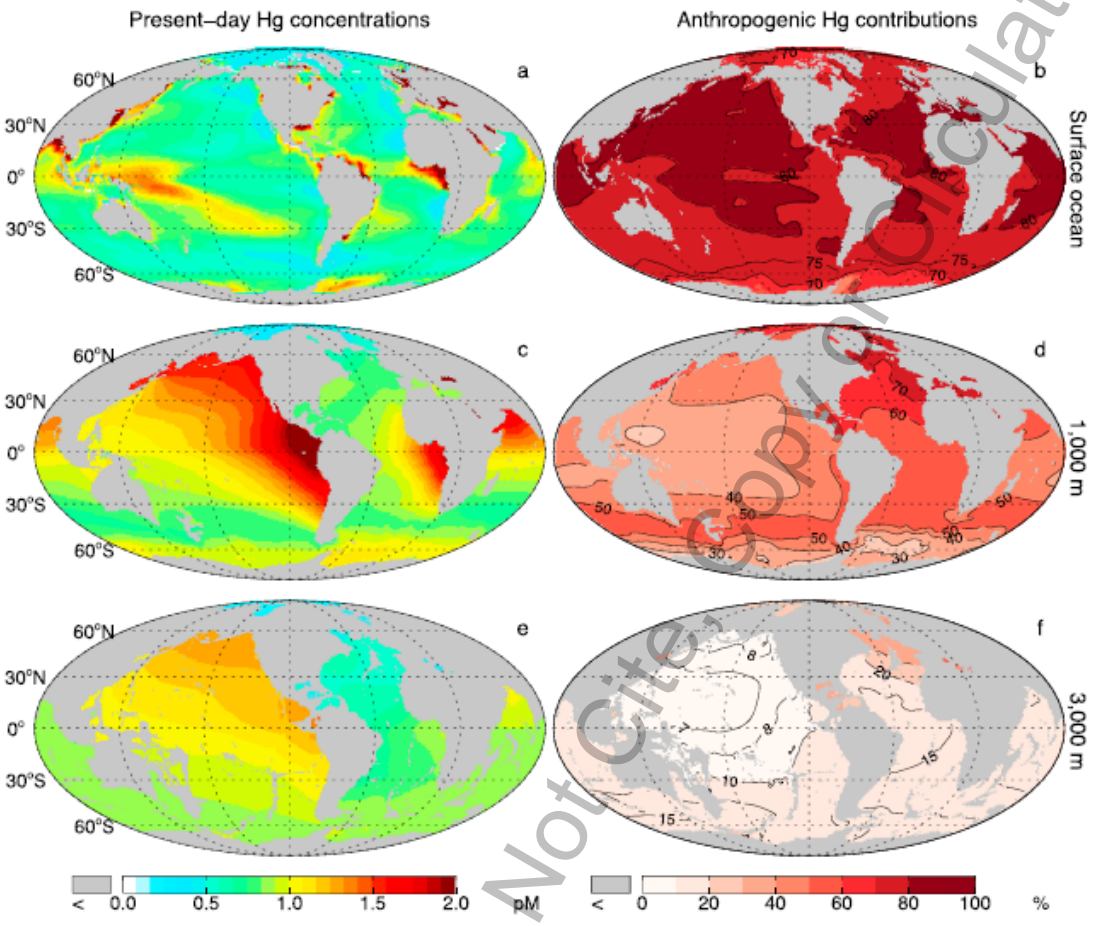

Figure 3. Spatial distribution of Hg concentrations in the present-day ocean. Annual mean concentrations of total Hg (in pM) for (a) the mixed layer, (c) 1000 m depth, and (e) 3000 m depth. (b, d, and f) Contributions of anthropogenic Hg to the present-day concentrations, expressed in percentage.

Figure 1.2.6. Inter-basin and vertical distribution of total Hg concentrations, and the fraction of anthropogenic Hg, in today's oceans. Use caption shown, but figure will be redrawn. from Zhang et al. 2014 GBC.

1.3 References

AMAP/UNEP 2013. Technical Background Report for the Global Mercury Assessment 2013. Arctic Monitoring and Assessment Programme, Oslo, Norway / UNEP Chemicals Branch, Geneva, Switzerland. 263 p.

Amos, H. M.; Jacob, D. J.; Kocman, D.; Horowitz, H. M.; Zhang, Y.; Dutkiewicz, S.; Horvat, M.; Corbitt, E. S.; Krabbenhoft, D. P.; Sunderland, E. M. 2014. Global biogeochemical implications of mercury discharges from rivers and sediment burial. Environ. Sci. Technol. 48: 9514–9522.

Amos, H. M.; Jacob, D. J.; Streets, D. G.; Sunderland, E. M. 2013. Legacy impacts of all-time anthropogenic emissions on the global mercury cycle. Global Biogeochem. Cycles 27: 410−421.

Amos HM, Sonke JE, Obrist D, Robins N, Hagan N, Horowitz HM, Mason RP, Witt M, Hedgecock IM, Corbitt ES, Sunderland EM. 2015. Observational and modeling constraints on global anthropogenic enrichment of mercury. Environ. Sci. Technol. 49:4036-4047. doi:10.1021/es5058665.

Bagnato E, Tamburello G, Avard G, Martinez-Cruz M, Enrico M, Fu X, et al. 2014. Mercury fluxes from volcanic and geothermal sources: an update. In: Zellmer GF, Edmonds M, Straub SM, editors. The Role of Volatiles in the Genesis, Evolution and Eruption of Arc Magmas. Special Publications, 410. Geological Society, London.

Beal SA, Osterberg EC, Zdanowicz CM, Fisher DA. 2015. Ice core perspective on mercury pollution during the past 600 years. Environ. Sci. Technol. 49, 7641−7647, doi: 10.1021/acs.est.5b01033.

Black, F. J., A. Paytan, K. L. Knee, N. R. De Sieyes, P. M. Ganguli, E. Gary and A. R. Flegal (2009). Submarine Groundwater Discharge of Total Mercury and Monomethylmercury to Central California Coastal Waters. Environmental Science & Technology **43**: 5652-5659.

Bone, S. E., M. A. Charette, C. H. Lamborg and M. E. Gonneea (2007). Has Submarine Groundwater Discharge Been Overlooked as a Source of Mercury to Coastal Waters? Environmental Science & Technology **41**: 3090-3095.

Bowman KL, Hammerschmidt CR, Lamborg CH, Swarr G. 2015. Mercury in the North Atlantic Ocean: The U.S. GEOTRACES zonal and meridional sections. *Deep-Sea Res. II* **116**: 251-261.

Bowman KL, Hammerschmidt CR, Lamborg CH, Swarr GJ, Agather AM. 2016. Distribution of mercury species across a zonal section of the eastern tropical South Pacific Ocean (U.S. GEOTRACES GP16). *Mar.Chem.* **186**: 156-166.

Cooke, C. A.; Hintelmann, H.; Ague, J. J.; Burger, R.; Biester, H.; Sachs, J. P.; Engstrom, D. R. Use and Legacy of mercury in the Andes. Environ. Sci. Technol. 2013, 47 (9), 4181−4188.

Correla J.P., Valero-Garces, BL, Wang F, Martínez-Cortizas A, Cuevas CA, and Saiz-Lopez, A. 2017. 700 years reconstruction of mercury and lead atmospheric deposition in the Pyrenees (NE Spain). Atmospheric Environment 155: 97-107.

Engstrom, D. R.; Fitzgerald, W. F.; Cooke, C. A.; Lamborg, C. H.; Drevnick, P. E.; Swain, E. B.; Balogh, S. J.; Balcom, P. H. 2014. Atmospheric Hg emissions from preindustrial gold and silver extraction in the Americas: A reevaluation from lake-sediment archives. Environ. Sci. Technol. 48: 6533−6543.

Ferrara R, Mazzolai B, Lanzillotta E, Nucaro E, Pirrone N. Volcanoes as emission sources of atmospheric mercury in the Mediterranean basin. Sci. Total Environ. 2000; 259: 115–121.

Fu X, Zhu W, Zhang H, Sommar J, Yu B, Yang X, Wang X, Lin C-J, and Feng X. 2016. Depletion of atmospheric gaseous elemental mercury by plant uptake at Mt. Changbai, Northeast China. Atmos Chem Phys 16: 12861–12873. doi:10.5194/acp-16-12861-2016

Ganguli, P. M., C. H. Conaway, P. W. Swarzenski, J. A. Izbicki and A. R. Flegal (2012). Mercury Speciation and Transport via Submarine Groundwater Discharge at a Southern California Coastal Lagoon System. Environmental Science & Technology **46**: 1480-1488.

German, C. R., K. A. Casciotti, J.-C. Dutay, L. E. Heimbürger, W. J. Jenkins, C. I. Measures, R. A. Mills, H. Obata, R. Schlitzer, A. Tagliabue, D. R. Turner and H. Whitby (2016). Hydrothermal impacts on trace element and isotope ocean biogeochemistry. Philosophical Transactions of the Royal Society A: Mathematical, Physical and Engineering Sciences **374**(2081).

Guerrero, S. 2012. Chemistry as a tool for historical research: Identifying paths of historical mercury pollution in the Hispanic New World. Bull. Hist. Chem. 37: 61−70.

Horowitz, H. M.; Jacob, D. J.; Amos, H. M.; Streets, D. G.; Sunderland, E. M. 2014. Historical mercury releases from commercial products: Global environmental implications. Environ. Sci. Technol. 48: 10242−10250.

Kang S., Huang J., Wang F., Zhang Q., Zhang Y., Li C., Wang L., Chen P., Sharma C., Li Q., Sillanpää M., Hou J., Xu B., and Guo J., 2016. Atmospheric mercury depositional chronology reconstructed from lake sediment and ice cores in the Himalayas and Tibetan Plateau. Environ. Sci. Technol., 50, 2859–2869

Lamborg, C. H., C. R. Hammerschmidt and K. L. Bowman (2016). An examination of the role of particles in oceanic mercury cycling. Philosophical Transactions of the Royal Society A: Mathematical, Physical and Engineering Sciences 374 (2081), doi: 10.1098/rsta.2015.0297

Lamborg, C. H., Fitzgerald, W. F., O'Donnell, J. & Torgersen, T. A non-steady-state compartmental model of global-scale mercury biogeochemistry with interhemispheric atmospheric gradients. Geochim. Cosmochim. Acta 66: 1105–1118 (2002).

Lamborg, C. H.; Hammerschmidt, C. R.; Bowman, K. L.; Swarr, G. J.; Munson, K. M.; Ohnemus, D. C.; Lam, P. J.; Heimbürger, L. E.; Rijkenberg, M. J. A.; Saito, M. A. 2014. A global ocean inventory of anthropogenic mercury based on water column measurements. Nature 512: 65−68.

Lamborg, C. H., K. L. Von Damm, W. F. Fitzgerald, C. R. Hammerschmidt and R. Zierenberg (2006). Mercury and monomethylmercury in fluids from Sea Cliff submarine hydrothermal field, Gorda Ridge. Geophys. Res. Lett. **33**(17): L17606.

Laurier, F. J. G., D. Cossa, C. Beucher and E. Breviere (2007). The impact of groundwater discharges on mercury partitioning, speciation and bioavailability to mussels in a coastal zone. Marine Chemistry 104: 143-155.

Lee, Y.-G., M. D. M. Rahman, G. Kim and S. Han (2011). Mass Balance of Total Mercury and Monomethylmercury in Coastal Embayments of a Volcanic Island: Significance of Submarine Groundwater Discharge. Environmental Science & Technology 45: 9891-9900.

Liu M, Zhang W, Wang X, Chen L, Wang H, Luo Y, Zhang H, Shen H, Tong Y, Ou L, Xie H, Ye X, and Deng C. 2016. Mercury Release to Aquatic Environments from Anthropogenic Sources in China from 2001 to 2012.Environ Sci Technol *50*: 8169–8177. doi: 10.1021/acs.est.6b01386

Mason, R. P., A. L. Choi, W. F. Fitzgerald, C. R. Hammerschmidt, C. H. Lamborg, A. L. Soerensen, and E. M. Sunderland. (2012) Mercury biogeochemical cycling in the ocean and policy implications. Environ. Res., 119: 101–117. doi:10.1016/j.envres.2012.03.013.

Mason, R. P.; Fitzgerald, W. F.; Morel, F. M. M. 1994. The biogeochemical cycling of element mercury - Anthropogenic influences. Geochim. Cosmochim. Acta 58: 3191−3198.

Melitza Crespo-Medina, A. D. Chatziefthimiou and N. S. Bloom (2009). Adaptation of chemosynthetic microorganisms to elevated mercury concentrations in deep-sea hydrothermal vents. Limnology and Oceanography **54**: 41-49.

Nriagu J, Becker C. 2003. Volcanic emissions of mercury to the atmosphere: global and regional inventories. Sci. Total Environ. 304: 3–12.

Nriagu JO. 1989. A global assessment of natural sources of atmospheric trace metals. Nature 338: 47-49.

Nriagu, J. O. (1993). Legacy of mercury pollution. Nature 363, 589.

Obrist D, Agnan Y, Jiskra M, Olson CL, Colegrove DP, Hueber J, Moore CW, Sonke JE, and Helmig D. 2017. Tundra uptake of atmospheric elemental mercury drives Arctic mercury pollution. Nature 547: 201-204.

Pyle, D. M., and T. A. Mather. 2003. The importance of volcanic emissions for the global atmospheric mercury cycle. Atmos. Env. 37, 5115-5124.

Schuster, P. F.; Krabbenhoft, D. P.; Naftz, D. L.; Cecil, L. D.; Olson, M. L.; Dewild, J. F.; Susong, D. D.; Green, J. R.; Abbott, M. L. Atmospheric mercury deposition during the last 270 years: A glacial ice core record of natural and anthropogenic sources. Environ. Sci. Technol. 2002, 36 (11), 2303−2310.

Selin, N. E. et al. 2008. Global 3-D land-ocean-atmosphere model for mercury: present day versus preindustrial cycles and anthropogenic enrichment factors for deposition. Glob. Biogeochem. Cycles 22, GB2011.

Selin, N. E. Global change and mercury cycling: Challenges for implementing a global mercury treaty. Environ. Toxicol. Chem. 2013, DOI: 10.1002etc.237.

Sherman, L. S., J. D. Blum, D. K. Nordstrom, R. B. McCleskey, T. Barkay and C. Vetriani (2009). Mercury isotopic composition of hydrothermal systems in the Yellowstone Plateau volcanic field and Guaymas Basin sea-floor rift." Earth and Planetary Science Letters 279: 86-96.

Sonke, J. E., L.-E. Heimbürger and A. Dommergue (2013). Mercury biogeochemistry: Paradigm shifts, outstanding issues and research needs. Comptes Rendus Geoscience 345: 213-224

Soerensen, A. L. et al. 2010. An improved global model for air-sea exchange of mercury: high concentrations over the North Atlantic. Environ. Sci. Technol. 44, 8574–8580.

Song S, Selin NE, Soerensen AL, Angot H, Artz R, et al 2015. Top-down constraints on atmospheric mercury emissions and implications for global biogeochemical cycling. Atmos. Chem Phys. 15: 7103-7125.

Streets DG, Horowitz HM, Jacob DJ, Lu Z, Levin L, ter Schure AFH, and Sunderland EM. 2017. Total mercury released to the environment by human activities. Environ. Sci Technol. doi: 10.1021/acs.est.7b00451.

Streets, D. G.; Devane, M. K.; Lu, Z. F.; Bond, T. C.; Sunderland, E. M.; Jacob, D. J. 2011. All-time releases of mercury to the atmosphere from human activities. Environ. Sci. Technol. 45: 10485−10491.

Strode, S., Jaegle, L. & Emerson, S. Vertical transport of anthropogenic mercury in the ocean. Glob. Biogeochem. Cycles 24, GB4014 (2010).

Strode, S., L. Jaeglé, and N. E. Selin (2009), Impact of mercury emissions from historic gold and silver mining: Global modeling, Atmos. Environ., 43, 2012–2017.

Sunderland EM, and Selin NE. 2013. Future trends in environmental mercury concentrations: implications for prevention strategies. *Environmental Health* **12**, doi**:** 10.1186/1476-069X-12-2.

Sunderland, E. M.; Mason, R. P. 2007. Human impacts on open ocean mercury concentrations. Global Biogeochem. Cycles 21 (4), No. GB4022.

Wang X, Bao **Z**, Lin C-J, Yuan W, and Feng X. 2016. Assessment of Global Mercury Deposition through Litterfall. *Environ. Sci. Technol. 50*: 8548–8557. doi: 10.1021/acs.est.5b06351.

Zhang, Y., Jacob, D.J., Horowitz, H.M., Chen, L., Amos, H.M., Krabbenhoft, D.P. Slemr, F., St. Louis, V.L., and Sunderland, E.M. 2016. Observed decrease in atmospheric mercury explained by global decline in atmospheric emissions. Proc. Nat. Acad. Sci., doi:10.1073/pnas.1516312113.

Zhang, Y.; Jaeglé, L.; Thompson, L.; Streets, D. 2014. Six centuries of changing oceanic mercury. Global Biogeochem. Cycles No. 2014GB004939.

Zheng, J. 2015. Archives of total mercury reconstructed with ice and snow from Greenland and the Canadian High Arctic. Sci. Total Environ. 509–510: 133–144.